

# ChemComm

Chemical Communications

Accepted Manuscript

This article can be cited before page numbers have been issued, to do this please use: T. Tian, T. Qian, T. Jiang, Y. Deng, X. Li, W. Yuan, Y. Chen, Y. Wang and W. Hu, *Chem. Commun.*, 2020, DOI: 10.1039/D0CC01350A.



This is an Accepted Manuscript, which has been through the Royal Society of Chemistry peer review process and has been accepted for publication.

Accepted Manuscripts are published online shortly after acceptance, before technical editing, formatting and proof reading. Using this free service, authors can make their results available to the community, in citable form, before we publish the edited article. We will replace this Accepted Manuscript with the edited and formatted Advance Article as soon as it is available.

You can find more information about Accepted Manuscripts in the [Information for Authors](#).

Please note that technical editing may introduce minor changes to the text and/or graphics, which may alter content. The journal's standard [Terms & Conditions](#) and the [Ethical guidelines](#) still apply. In no event shall the Royal Society of Chemistry be held responsible for any errors or omissions in this Accepted Manuscript or any consequences arising from the use of any information it contains.

## COMMUNICATION

## A Donor-Acceptor Type Macrocyclic: Toward Photolyzable Self-Assembly

Received 00th January 20xx,  
Accepted 00th January 20xx

DOI: 10.1039/x0xx00000x

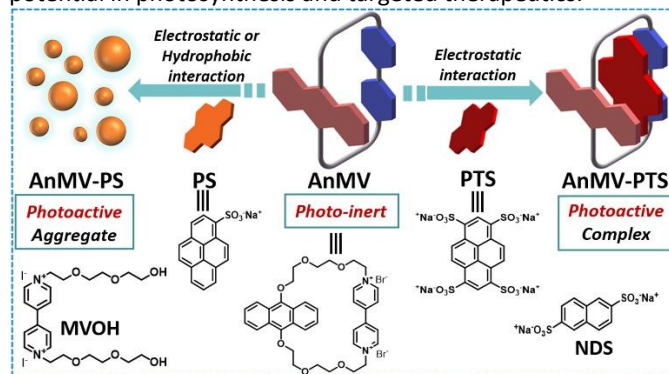
Tian Tian,<sup>a</sup> Tingjuan Qian,<sup>a</sup> Tingting Jiang,<sup>a</sup> Yakui Deng,<sup>a</sup> Xiaopei Li,<sup>a</sup> Wei Yuan,<sup>a</sup> Yulan Chen,<sup>\*a,b</sup> Yi-Xuan Wang,<sup>\*a,b</sup> and Wenping Hu<sup>a,b</sup>

A water-soluble macrocyclic host is reported, composed of alkoxyanthracene as donor (D), and 4,4-bipyridinium as acceptor (A). Intramolecular D-A structure renders the host highly photostable. However, the introduction of strong electron-donating guest promotes the photodecomposition of alkoxyanthracene, yielding photolyzable host-guest complexes or aggregates.

The development of photo-decomposable structure had derived a series of degradable materials,<sup>1</sup> and targeted delivery vehicles.<sup>2</sup> Supramolecular self-assembly based on macrocyclic compound possessed the inherent advantage in the fabrication of photodegradable systems. The non-covalent binding, between macrocyclic host and guest molecule, makes the association highly dynamic, which can be easily disrupted. Numerous host-guest pairs have been employed in photodegradable systems, most of which rely on photoactive guests and traditional macrocycles.<sup>3</sup> However, such systems may not show the complete photolysis because most macrocycles are reserved after irradiation, which can bind with decomposed guests to form new assemblies. Meanwhile, photo-responsive macrocyclic hosts have not been fully developed due to the complicated synthesis, and the steric inhibition of photo-isomerization by ring strain and molecular crowding.<sup>4</sup> Hence, the development of the macrocyclic compounds with efficient photoreactivity has become an urgent requirement for photodegradable supramolecular systems. Recently, macrocyclic hosts based on photo-isomerized bridging subunits were developed, which showed excellent photo-controlled guest release.<sup>5</sup> As a matter of fact, there also reminded a need for the development of thoroughly

photodecomposable macrocycles for enriching the photolyzable host-guest systems.

In our previous work, a new strategy for construction of photodegradable materials has been proposed, that is, supramolecular self-assembly induced photolysis.<sup>6</sup> Alkoxyanthracene derivatives were selected as the photolyzable guests,<sup>7</sup> and their photo-reactivities were enhanced upon addition of macrocycles, yielding highly photoactive assemblies. Inspired by the success, a potentially photolyzable and water-soluble macrocycle (AnMV) was designed and synthesized, which consists of a photo-responsive alkoxyanthracene (An) unit and a dicationic 4,4-bipyridinium (MV) unit (Scheme 1). The electron-deficient MV, which is closely anchored within the macrocycle, extinguished the photoactivity of An, making the macrocyclic host photo-inert. Moreover, the introduction of strong electron-donating guest replaced the intramolecular donor (D)-acceptor (A) interaction with the intermolecular D-A interaction, and thereby freed An unit for efficient photodecomposition. Additionally, host-guest nanoaggregate on the basis of AnMV can be fabricated by altering the hydrophilicity of guest. The present study provides pioneering proof of principle for smart self-assembly systems based on photolyzable macrocyclic hosts, which will show great potential in photosynthesis and targeted therapeutics.<sup>8a</sup>



**Scheme 1.** Self-assembly modes of AnMV with different guests, and the chemical structures of all the substances in this work.

<sup>a</sup> Tianjin Key Laboratory of Molecular Optoelectronic Sciences, Department of Chemistry, School of Science, Tianjin University, Tianjin 300072, China  
E-mail: yulan.chen@tju.edu.cn, yx\_wang@tju.edu.cn

<sup>b</sup> Collaborative Innovation Center of Chemical Science and Engineering (Tianjin), Tianjin 300072, P. R. China

† Electronic Supplementary Information (ESI) available.

See DOI: 10.1039/x0xx00000x

1,3,6,8-Pyrenetetrasulfonic acid tetrasodium salt (**PTS**) was selected to be the guest molecule because it can be easily associated with positively charged **AnMV**, and its strong electron-donating ability is beneficial to mediate the D-A interaction.<sup>9</sup> UV-vis absorption spectroscopy was performed to monitor the D-A interaction of the host-guest system. It was clearly shown in Figure 1a that **AnMV** and **AnMV-PTS** had distinctly different absorption band between 500 nm and 700 nm, providing the evidence for the forming of new CT interaction between **PTS** and **AnMV**.<sup>8a</sup> Compared with the **AnMV** ( $\lambda_{\text{max}} = 525$  nm), the maximum absorption band of **AnMV-PTS** complex exhibited a bathochromic shift ( $\lambda_{\text{max}} = 550$  nm) with increased intensity, indicating that the CT interaction of **AnMV-PTS** complex was stronger than that of **AnMV** itself.<sup>10</sup> Such spectral change can also be easily observed by naked eye (Figure S1). On the contrary, the noncyclic control compound, **MVOH**, did not show CT absorption above 500 nm in the presence of **PTS**, implying that the regulation of D-A interaction cannot be achieved without macrocyclic structure. Fluorescence spectroscopy was also used to testify the evolution of D-A interactions.<sup>11</sup> The emission intensity of **PTS** was decreased by 80% after binding with **AnMV** (Figure 1b), ascribed to the photo electron transfer (PET) between **PTS** and **MV** unit.<sup>12</sup> Meanwhile, only 32% of fluorescence was quenched with **MVOH**, again revealing the essential role of macrocyclic structure in the intermolecular interaction. We further demonstrated the formation of **AnMV-PTS** complex by cyclic voltammetry experiments. As shown in Figure S2a, redox peaks of **MV** moieties in **AnMV-PTS** complex were different with those in free **AnMV**. However, redox peaks of **MVOH** had almost no change in the presence of **PTS**, suggesting that the electrostatic interaction between **MVOH** and **PTS** was too weak to yield CT complex (Figure S2b). All these results proved that the **PTS** was successfully incorporated with cyclic **AnMV**, and replaced the intramolecular CT interaction of **AnMV** itself with the intermolecular CT interaction between **AnMV** and **PTS**.

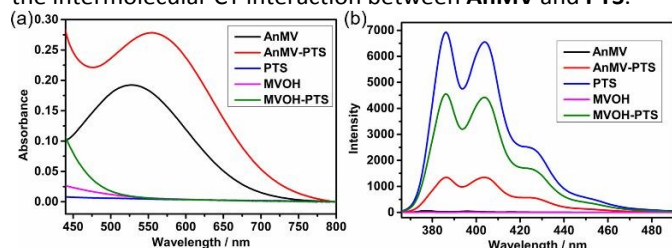


**Figure 1.** (a) UV-vis absorption spectra, and (b) fluorescence spectra ( $\lambda_{\text{ex}} = 365$  nm) of **PTS**, **AnMV-PTS**, **AnMV**, **MVOH**, and **MVOH-PTS** in water. The concentrations of all the constituents were 0.5 mM in UV-vis experiments, and 0.01 mM in fluorescence experiments.

NMR experiments were performed for detailed information about the host-guest binding behavior in the solution state. Compared with those in free **AnMV**, all the protons of **AnMV** underwent upfield resonance shifts in the presence of **PTS** (Figure 2a), due to the ring current effect of the aromatic nuclei of pyrene, confirming the spatial correlation between two components.<sup>10,13</sup> The **PTS** protons also showed visible upfield

shifts for the same reason. As a control, protons of **MV** units in acyclic **MVOH** underwent smaller upfield resonance shifts with **PTS** (Figure S4), again indicating the weaker interaction between **PTS** and **MVOH**. Job plot was obtained to determine the binding stoichiometry. A peak at the molar fraction of 0.5 was observed (Figures S5), verifying a 1:1 (or n:n) binding between **AnMV** and **PTS**.<sup>14</sup> The diffusion coefficients of **AnMV-PTS** complex, **AnMV** and **PTS** were measured by the diffusion-ordered spectroscopy (DOSY). When **PTS** was added to **AnMV** aqueous solution, the diffusion coefficient was decreased from  $2.88 \times 10^{-10}$  to  $2.00 \times 10^{-10}$   $\text{m}^2\text{s}^{-1}$ , and protons from both components showed similar coefficients, meaning that one primary complex was formed with slower diffusion (Table S1). According to the Stokes-Einstein equation, the hydrodynamic volume of **AnMV** was only increased by 2.90 times after addition of **PTS**,<sup>15</sup> which can preclude the possibility of n:n **AnMV-PTS** aggregation. Therefore, we can confirm a 1:1 binding stoichiometry for **AnMV-PTS** complex in solution. Furthermore, binding affinity was quantitatively studied via <sup>1</sup>H NMR titration experiment. The association constant ( $K_a$ ) is determined, by the nonlinear curve simulation, as  $(4.77 \pm 0.35) \times 10^4$   $\text{M}^{-1}$  (Figures S6), which illustrated the strong binding ability of **AnMV** to **PTS**. 2,6-Naphthalenedisulfonic acid disodium salt (**NDS**) was also selected as a guest for **AnMV** to study the effect of guest structure on host-guest complexation. As shown in Figure S7, the CT absorption of **AnMV** only slightly changed when a large amount of **NDS** was added, implying a much less sufficient regulation on CT interaction by **NDS**. A significant decrease in the association constant was also found ( $K_a = (154 \pm 25) \text{M}^{-1}$  for **AnMV-NDS** complex, Figure S8), suggesting that smaller aromatic core of guest molecule might significantly reduce the association ability.<sup>5a</sup>

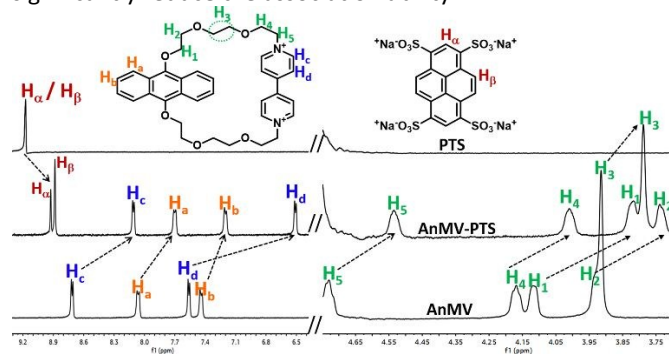


**Figure 2.** Partial <sup>1</sup>H NMR spectra of **PTS**, **AnMV-PTS** complex, and **AnMV** (400 MHz, 0.5 mM).

2D NOESY NMR spectrum was further utilized to explore the binding geometry of **AnMV** with **PTS**. The NOE correlation of  $H_{\alpha}$  of **PTS** with  $H_3$  of the glycol chain, and correlations of  $H_{\beta}$  of **PTS** with protons of **An** and **MV**, were clearly observed (Figure S9b and S9c), jointly suggesting that the pyrene segment was embedded in the macrocycle, and was oriented parallelly with the **MV** segment. Combined with the conclusions from 1D NMR experiments, the geometric structure of complex was deduced (Figure S9d,e), which was further verified by DFT calculations (Figure S10). The complexation in the solid state was also studied by XRD analysis of the single crystal of 1:1 **AnMV-PTS**

complex. As displayed in Figure 3, **PTS** was located between **MV** and **An** units of the host, and adopted a parallel arrangement to **MV**, which revealed the mechanism of the regulation on intramolecular CT interaction by host–guest binding.<sup>16</sup> The close association (ca. 2.3 Å) of oxygen atoms of **PTS** with H<sub>c</sub>/H<sub>d</sub> of glycol chain and H<sub>a</sub> of **MV** was observed, resulting from the electrostatic interaction between sulfonate group and pyridinium.<sup>17</sup> Although pyrene was not fully embedded into the macrocyclic cavity in the densely packed crystal state, it is possible that **PTS** can be included into **AnMV** in the more flexible solution state in terms of their sizes and shapes.<sup>18</sup>

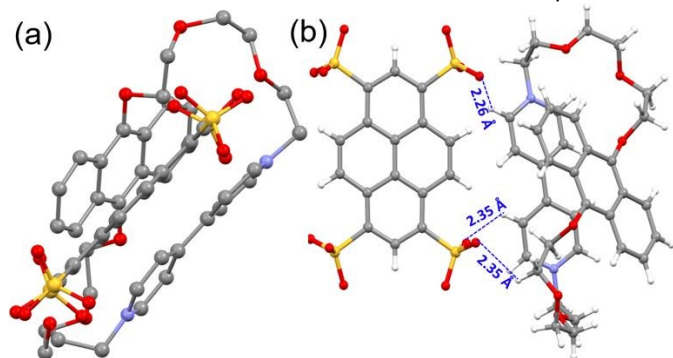


**Figure 3.** Solid-state (super)structure of **AnMV–PTS** complex obtained from X-ray crystallography on single crystal. The counterions and solvent molecules are omitted for the sake of clarity.

Combining all the results, we can conclude that there is CT interaction in **AnMV** itself, in which **An** units is the electron donor and **MV** group is the electron-acceptor. The addition of strong electron-donating guest will regulate the CT interaction through the encapsulation by macrocycle driven by electrostatic interaction.

9,10-Alkoxyanthracene is a typical photolytic unit.<sup>7</sup> It can be converted to endoperoxide (EPO) by singlet oxygen, generated from triplet oxygen under irradiation, and further decompose into 9,10-anthraquinone.<sup>8a</sup> The reactivity was highly dependent on the electron density of anthracene.<sup>19</sup> Herein, **An** unit in **AnMV** should be optically stable due to the D–A structure, but be photo-responsive with the electron-donating guest. UV–vis absorption at 405 nm was recorded to monitor the photolysis of **AnMV** and its host–guest complex, as **PTS** did not show intense absorption at this wavelength both before and after irradiation (Figure S11a). As shown in Figures 4a and S11b, the absorption of **AnMV** had almost no change after irradiation for 60 min, indicating the excellent photo-stability. In contrast, the absorption of **AnMV–PTS** complex at 405 nm decreased by 77% under the same condition. According to the  $K_a$ , 64% of **AnMV** was bound with **PTS** at the experimental concentration. Therefore, all the complexed **AnMV** had been decomposed, manifesting that the complex is highly photoactive. **NDS** was also tested as the guest molecule for comparison. As the  $K_a$  of **AnMV–NDS** complex was much smaller than that of **AnMV–PTS** complex, we used excess **NDS** to ensure the high complexation degree of **AnMV**. After addition of 500 eq of **NDS**, 88% of **AnMV** was complexed, but only 56% of **AnMV** was photo-decomposed (Figure S12). It clearly demonstrated that stronger electron-

donating ability of guest facilitated the photoactivity of the host–guest complex. The photolytic products of free **AnMV** and **AnMV–PTS** complex were identified by <sup>1</sup>H NMR, GC–MS and HR–EI–MS measurements. The irradiated mixture was purified via solvent extraction, and the results were consistent with those of proposed products (Figures S13–S15). It fully proved that **AnMV** underwent same photo-transformation as reported in the presence and absence of **PTS**, and excluded the possibility that the changes in photo-activity were derived from different reaction routes. In the light of results, we could conclude that a photostable macrocyclic host was successfully developed because of the efficient intramolecular CT interaction. The introduction of highly electron-rich guest inhibited the PET process from **An** to **MV** segments in host, and further enabled the photo-reactivity, making the host–guest complex photolyzable. Note that the specific signals of **PTS** in aqueous solution were observed after irradiation (Figure S16), implying that **PTS** was not destroyed during the photo-reaction. Therefore, such host–guest system could be potentially used as photo-degradable inclusion, which was widely applied in biotechnology and pharmacy.<sup>20</sup>

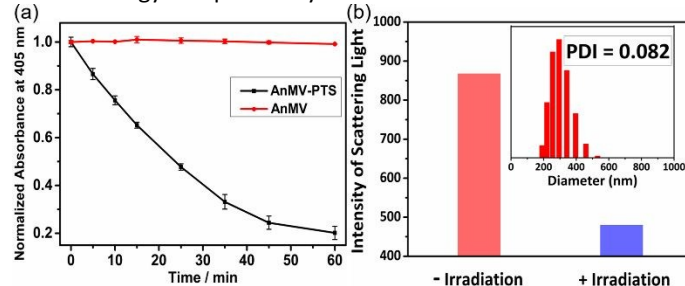


**Figure 4.** (a) Normalized absorbance at 405 nm of the free **AnMV**, and **AnMV–PTS** complex upon irradiation at 365 nm for different times. Error bars indicate SDs from three measurements for each point. (b) The intensities of dynamic laser scattering (DLS) light of **AnMV–PS** aggregates before and after irradiation. Inset: DLS data of **AnMV–PS** aggregate in water. Concentrations of all the substances were kept at 0.1 mM.

Stimulus-responsive nanoaggregates can be constructed by host–guest complexation, which have a wide range of application in environmental science, and biomedicine.<sup>21</sup> To our particular interest herein is that, 1:1 (molar ratio) mixture of **AnMV** and 1-pyrenesulfonic acid sodium salt (**PS**) in aqueous solution showed the Tyndall effect (Figure S17), which promoted us to explore the aggregation based on this host–guest self-assembly system. The critical aggregation concentration (CAC) of **AnMV** (0.15 mM) in the presence of **PS** was measured by monitoring the dependence of the optical transmittance at 710 nm on **PS** concentration. The optical transmittance decreased gradually as the concentration of **PS** increased because of the scattering effect of newly formed nanoscale assembly (Figure S18a), and the CAC was obtained as ca. 0.08 mM (Figures S18b). However, the optical transmittance of **AnMV** without **PS** at 710 nm showed no appreciable change as the concentration increased from 0.05 to 0.25 mM (Figure S19). Due to less sulfonate groups attached on pyrene core, **PS**

was more hydrophobic and was easier to stack than **PTS**, which leads to the complexation-induced aggregation.<sup>22</sup> Furthermore, dynamic laser scattering (DLS) and scanning electron microscope (SEM) were employed to identify the morphology of **AnMV–PS** assembly. DLS result showed that **AnMV–PS** complex formed aggregates with a narrow size distribution, giving an average diameter of 328 nm (Figure 4b). The SEM image (Figure S20a) revealed that the aggregates were nanospheres. We further explored the photodegradation of the supramolecular assembly. The UV–vis absorption of **AnMV–PS** assembly at 405 nm decreased significantly after irradiation (Figures S21 and S22), implying the efficient photodecomposition of **AnMV** in aggregate. The CT band for **AnMV–PS** complex showed a bathochromic shift with increased intensity, indicating that the photolysis was also because of the mediation on CT interaction of **AnMV**. In addition, the intensity of scattering light of aggregate pronouncedly decreased (Figure 4b), demonstrating the size and quantity of nanoaggregates were reduced. The spherical assemblies also disappeared in the SEM image (Figure S20b). We also Hence, we successfully constructed photodegradable nanoaggregates based on host–guest chemistry of **AnMV**.

In conclusion, a water-soluble macrocycle, **AnMV**, was designed and synthesized. The intramolecular D–A structure lowered the electron density of **An** segment, making **AnMV** photo-stable. However, when a strongly electron-donating guest (e.g., **PTS**) was introduced, it was embedded into the macrocyclic host, leading to increased electron density on **An** unit and considerably enhanced photo-decomposition of the complex. By adjusting the hydrophilicity of guest molecule, we could also obtain photodegradable nanoaggregates (**AnMV–PS**). This host–guest system provides a new train of thought for photo-responsive self-assemblies, and exhibits promising applications for photo-controlled drug delivery and molecular switching in the future.

This work was supported by the National Key Research and Development Program of China (Grants 2016YFB0401100) and the National Natural Science Foundation of China (Grants 21604062). The authors are grateful to Prof. Long Chen (Tianjin University) for his help with photoreaction measurements.

## Conflicts of interest

There are no conflicts to declare.

## Notes and references

- 1 Y. Wang, H. Xu and X. Zhang, *Adv. Mater.*, 2009, **21**, 2849–2864.
- 2 A. S. Lubbe, W. Szymanski and B. L. Feringa, *Chem. Soc. Rev.*, 2017, **46**, 1052–1079.
- 3 (a) J. Wang, H.-Y. Zhang, X.-J. Zhang, Z.-H. Song, X.-J. Zhao and Y. Liu, *Chem. Commun.*, 2015, **51**, 7329–7332; (b) Z. Liu, S. K. M. Nalluri and J. F. Stoddart, *Chem. Soc. Rev.*, 2017, **46**, 2459–2478; (c) G. Crini, *Chem. Rev.*, 2014, **114**, 10940–10975; (d) Y. Zhang, Y.-C. Pan, Y. Wang, D.-S. Guo, J. Gao and Z. Yang, *Nanoscale* 2018, **10**, 18829–18834; (e) J. W. Lee, S. Samal, N. Selvapalam, H.-J. Kim and K. Kim, *Acc. Chem. Res.*, 2003, **36**, 621–630; (f) J. del Barrio, S. T. J. Ryan, B. G. Jambrić, E. Rosta and O. A. Scherman, *J. Am. Chem. Soc.*, 2016, **138**, 5745–5748.
- 4 R. Reuter and H. A. Wegner, *Chem. Commun.*, 2011, **47**, 12267–12276.
- 5 (a) H. Wu, Y. Chen, L. Zhang, O. Anamimoghadam, D. Shen, Z. Liu, K. Cai, C. Pezzato, C. L. Stern, Y. Liu and J. F. Stoddart, *J. Am. Chem. Soc.*, 2019, **141**, 1280–1289; (b) X. Chi, W. Cen, J. A. Queenan, L. Long, V. M. Lynch, N. M. Khashab and J. L. Sessler, *J. Am. Chem. Soc.*, 2019, **141**, 6468–6472.
- 6 (a) Y.-X. Wang, Y.-M. Zhang and Y. Liu, *J. Am. Chem. Soc.*, 2015, **137**, 4543–4549; (b) T. Qian, F. Chen, Y. Chen, Y.-X. Wang and W. Hu, *Chem. Commun.*, 2017, **53**, 11822–11825.
- 7 (a) W. Fudickar and T. Linker, *J. Am. Chem. Soc.*, 2012, **134**, 15071–15082; (b) T. Yamamoto, S. Yagyu and Y. Tezuka, *J. Am. Chem. Soc.*, 2016, **138**, 3904–3911.
- 8 (a) K. Liu, C. Wang, Z. Li and X. Zhang, *Angew. Chem., Int. Ed.*, 2011, **50**, 4952–4956; (b) I. Roy, S. Bobbala, J. Zhou, M. T. Nguyen, S. K. M. Nalluri, Y. Wu, D. P. Ferris, E. A. Scott, M. R. Wasielewski and J. F. Stoddart, *J. Am. Chem. Soc.*, 2018, **140**, 7206–7212.
- 9 A. Das and S. Ghosh, *Angew. Chem., Int. Ed.*, 2014, **53**, 2038–2054.
- 10 Y. Jiao, J.-F. Xu, Z. Wang and X. Zhang, *ACS Appl. Mater. Interfaces*, 2017, **9**, 22635–22640.
- 11 K. Debsharma, J. Santhi, B. Baire and E. Prasad, *ACS Appl. Mater. Interfaces*, 2019, **11**, 48249–48260.
- 12 (a) P. Mukhopadhyay, Y. Iwashita, M. Shirakawa, S.-I. Kawano, N. Fujita and S. Shinkai, *Angew. Chem., Int. Ed.*, 2006, **45**, 1592–1595; (b) L. Chen, Y. Jiang, H. Nie, R. Hu, H. S. Kwok, F. Huang, A. Qin, Z. Zhao and B. Z. Tang, *ACS Appl. Mater. Interfaces*, 2014, **6**, 17215–17225; (c) H.-J. Kim, J. Heo, W. S. Jeon, E. Lee, J. Kim, S. Sakamoto, K. Yamaguchi and K. Kim, *Angew. Chem., Int. Ed.*, 2001, **40**, 1526–1529.
- 13 Detailed assignments of NMR signals for **AnMV** are shown in Figure S3.
- 14 H.-X. Zhao, D.-S. Guo and Y. Liu, *J. Phys. Chem. B*, 2013, **117**, 1978–1987.
- 15 Y. Cohen, L. Avram and L. Frish, *Angew. Chem., Int. Ed.*, 2005, **44**, 520–554.
- 16 M. Frasconi, I. R. Fernando, Y. Wu, Z. Liu, W.-G. Liu, S. M. Dyar, G. Barin, M. R. Wasielewski, W. A. Goddard and J. F. Stoddart, *J. Am. Chem. Soc.*, 2015, **137**, 11057–11068.
- 17 A. S. Jalilov, S. Patwardhan, A. Singh, T. Simeon, A. A. Sarjeant, G. C. Schatz and F. D. Lewis, *J. Phys. Chem. B*, 2014, **118**, 125–133.
- 18 G. Yu, C. Y. Han, Z. B. Zhang, J. Z. Chen, X. Z. Yan, B. Zheng, S. Y. Liu and F. H. Huang, *J. Am. Chem. Soc.*, 2012, **134**, 8711–8717.
- 19 (a) T. Yamamoto, S. Yagyu and Y. Tezuka, *J. Am. Chem. Soc.*, 2016, **138**, 3904–3911; (b) H. Qu, W. Cui, J. Li, J. Shao and C. Chi, *Org. Lett.*, 2011, **13**, 924–927.
- 20 (a) J.-H. Liu, X. Wu, Y.-M. Zhang and Y. Liu, *Asian J. Org. Chem.*, 2018, **7**, 2444–2447; (b) M. Hao, G. Sun, M. Zuo, Z. Xu, Y. Chen, X.-Y. Hu and L. Wang, *Angew. Chem., Int. Ed.*, 2019, **58**, 2–8.
- 21 (a) X. Yan, F. Wang, B. Zheng and F. Huang, *Chem. Soc. Rev.*, 2012, **41**, 6042–6065; (b) H. Wu, Y. Chen and Y. Liu, *Adv. Mater.*, 2017, **29**, 1605271; (c) G. Sun, Z. He, M. Hao, Z. Xu, X.-Y. Hu, J.-J. Zhu and L. Wang, *Chem. Commun.*, 2019, **55**, 10892–10895.
- 22 H.-W. Tian, Y.-C. Liu and D.-S. Guo, *Mater. Chem. Front.*, 2020, **4**, 46–98.

**Title:** A Donor-Acceptor Type Macrocyclic Host: Toward Photolyzable Self-Assembly

**Description:** A donor-acceptor macrocyclic host is reported, which showed efficient photodecomposition with electron-donating guests, yielding photolyzable host-guest complexes or aggregates.

**Graph:**